

# Hydrogen production from methane steam reforming over Ni on high surface area CeO<sub>2</sub> and CeO<sub>2</sub>-ZrO<sub>2</sub> supports synthesized by surfactant-assisted method

Thanaphon Palikanon<sup>1</sup>, Navadol Laosiripojana<sup>2</sup>,  
Suttichai Assabumrungrat<sup>3</sup> and Sumittra Charojrochkul<sup>4</sup>

## Abstract

Palikanon, T., Laosiripojana, N., Assabumrungrat, S. and Charojrochkul, S.  
Hydrogen production from methane steam reforming over Ni on  
high surface area CeO<sub>2</sub> and CeO<sub>2</sub>-ZrO<sub>2</sub> supports synthesized by  
surfactant-assisted method

Songklanakarin J. Sci. Technol., 2006, 28(6) : 1237-1249

Methane steam reforming performances of Ni on high surface area (HSA) CeO<sub>2</sub> and CeO<sub>2</sub>-ZrO<sub>2</sub> supports have been studied under solid oxide fuel cell (SOFC) operating conditions. Their performances were compared to general Ni/CeO<sub>2</sub>, Ni/CeO<sub>2</sub>-ZrO<sub>2</sub>, and Ni/Al<sub>2</sub>O<sub>3</sub>. It was firstly observed that Ni/CeO<sub>2</sub>-ZrO<sub>2</sub> (HSA) with the Ce/Zr ratio of 3/1 showed the best performance in terms of activity and stability toward the methane steam reforming among those with the Ce/Zr ratios of 1/1, 1/3, and 3/1. Both Ni/CeO<sub>2</sub>-ZrO<sub>2</sub> (HSA)

---

<sup>1</sup>M.Sc. student in Energy Technology, <sup>2</sup>Ph.D.(Chemical Engineering), The Joint Graduate School of Energy and Environment, King Mongkut's University of Technology Thonburi, Tungkrui Bangkok, 10140 Thailand.  
<sup>3</sup>Ph.D.(Chemical Engineering), Center of Excellence in Catalysis and Catalytic Reaction Engineering, Department of Chemical Engineering, Faculty of Engineering, Chulalongkorn University, Bangkok, 10330 Thailand.  
<sup>4</sup>Ph.D.(Material Science), National Metal and Materials Technology Center (MTEC), Thailand Science Park, Klong Luang, Pathum Thani, 12120 Thailand.

Corresponding e-mail: navadol\_1@jgsee.kmutt.ac.th  
Received, 24 January 2006 Accepted, 9 May 2006

and Ni/CeO<sub>2</sub> (HSA) presented better resistance toward carbon formation than the general Ni/CeO<sub>2</sub>, Ni/CeO<sub>2</sub>-ZrO<sub>2</sub>, and Ni/Al<sub>2</sub>O<sub>3</sub> at the same operating conditions. These benefits are related to the high oxygen storage capacity (OSC) of CeO<sub>2</sub>-ZrO<sub>2</sub>. During the steam reforming process, in addition to the reactions on Ni surface (\*), the redox reactions between the gaseous components presented in the system and the lattice oxygen (O<sub>x</sub>) on CeO<sub>2</sub>-ZrO<sub>2</sub> surface also take place. Among these reactions, the redox reactions between the high carbon formation potential compounds (CH<sub>4</sub>, CH<sub>x</sub>-\**n* and CO) and the lattice oxygen (O<sub>x</sub>) can prevent the formation of carbon species from the methane decomposition and Boudard reactions at the inlet H<sub>2</sub>O/CH<sub>4</sub> ratio of 3.0/1.0.

**Key words :** Methane steam reforming, carbon formation, high surface area, ceria, solid oxide fuel cell

### บทคัดย่อ

ธนพล ปาลีกันนท<sup>1</sup> นวต เหล่าศิริพจน์<sup>1</sup> สุทธิชัย อัสสะบำรุงรัตน์<sup>2</sup> และ สุมิตรา จรสโรจน์กุล<sup>3</sup>  
การผลิตไฮโดรเจนจากกระบวนการรีฟอร์มมิงของมีเทนด้วยไอน้ำบนตัวเร่งปฏิกิริยา Ni  
บนตัวรองรับ CeO และ CeO-ZrO ที่เตรียมขึ้นจากวิธี Surfactant-Assisted  
ว. สงขลานครินทร์ วท. 2549 28(6) : 1237-1249

การศึกษาตัวเร่งปฏิกิริยา นิกเกิล (Ni) บนตัวรองรับซีเรีย (CeO<sub>2</sub>) และซีเรียซีโครเนีย (CeO<sub>2</sub>-ZrO<sub>2</sub>) ที่เตรียมด้วยวิธี surfactant assisted (Ni/CeO (HSA), Ni/CeO<sub>2</sub>-ZrO<sub>2</sub> (HSA)) ทำได้โดยการเปรียบเทียบประสิทธิภาพในการแปรรูปมีเทนด้วยไอน้ำภายใต้สภาวะที่ใช้ในเซลล์เชื้อเพลิงแบบออกไซด์ของแข็ง (SOFC) กับตัวเร่งปฏิกิริยา Ni/CeO<sub>2</sub>, Ni/CeO<sub>2</sub>-ZrO<sub>2</sub>, and Ni/Al<sub>2</sub>O<sub>3</sub> ที่เตรียมด้วยวิธีทั่วไป จากการทดลองพบว่าตัวเร่งปฏิกิริยาชนิด Ni/CeO<sub>2</sub>-ZrO<sub>2</sub> (HSA) ณ ที่อัตราส่วน Ce/Zr เป็น 1/3 มีประสิทธิภาพในการเร่ง และคงสภาพการเกิดปฏิกิริยาการแปรรูปมีเทนด้วยไอน้ำมากที่สุดเมื่อเทียบกับ Ce/Zr ที่อัตราส่วนอื่น ๆ (1/1 และ 3/1) นอกจากนี้ตัวเร่งปฏิกิริยาที่ถูกเตรียมด้วยวิธี surfactant assisted ยังมีประสิทธิภาพในการต้านทานการเกิดคาร์บอน (carbon formation) ภายใต้สภาวะเดียวกันดีกว่าตัวเร่งปฏิกิริยาที่เตรียมด้วยวิธีทั่วไป ทั้งนี้เนื่องจากสมบัติพิเศษข้อนี้เป็นผลเนื่องมาจากความสามารถในการกักเก็บออกซิเจน (high oxygen storage capacity (OSC)) ที่ดีของตัวรองรับ CeO<sub>2</sub>-ZrO<sub>2</sub> โดยสมบัตินี้จะทำให้เกิดปฏิกิริยา redox (redox properties) ระหว่าง สารประกอบภายนอก (CH<sub>4</sub>, CH<sub>x</sub>-\**n* and CO) กับออกซิเจนที่ถูกปลดปล่อยออกมา (lattice oxygen (O<sub>x</sub>)) ซึ่งจะเป็นการลดการเกิดคาร์บอนบนพื้นผิวของตัวเร่งปฏิกิริยาอันเนื่องมาจากการแตกตัวของมีเทน และยังป้องกันการเกิดปฏิกิริยา Boudard ด้วย

<sup>1</sup>บัณฑิตวิทยาลัยร่วมด้านพลังงานและสิ่งแวดล้อม มหาวิทยาลัยเทคโนโลยีพระจอมเกล้าธนบุรี บางมด กรุงเทพฯ 10140 <sup>2</sup>ศูนย์เชี่ยวชาญทางเฉพาะทางด้านคาตาไลซิสและวิศวกรรมปฏิกิริยาที่ใช้ตัวเร่งปฏิกิริยา ภาควิชาวิศวกรรมเคมี คณะวิศวกรรมศาสตร์ จุฬาลงกรณ์มหาวิทยาลัย พญาไท กรุงเทพฯ 10330 <sup>3</sup>ศูนย์เทคโนโลยีโลหะและวัสดุแห่งชาติ อุทยานวิทยาศาสตร์แห่งประเทศไทย อำเภอลองหลวง จังหวัดปทุมธานี 12120

The methane steam reforming is a widely practised technology to produce hydrogen or synthesis gas for later utilization in solid oxide fuel cell (SOFC). Three main reactions are taken place as presented in the following equations.



Both water-gas shift reaction (Eq. 2) and reverse methanation (Eq. 3) are always associated with the steam reforming over a catalyst at elevated

temperatures. Due to the overall high endothermic nature of the reactions, these reactions are carried out at high temperature (700-900°C).

Commercial catalysts for the methane steam reforming reaction are nickel catalysts on supports such as  $\text{Al}_2\text{O}_3$ ,  $\text{MgO}$ ,  $\text{MgAl}_2\text{O}_4$  or their mixtures. Selection of a support material is an important issue as it has been evident that metal catalysts are not very active for the steam reforming when supported on inert oxides (Wang *et al.*, 2002). Various support materials have been tested, for example,  $\alpha\text{-Al}_2\text{O}_3$ ,  $\gamma\text{-Al}_2\text{O}_3$  and  $\gamma\text{-Al}_2\text{O}_3$  with alkali metal oxide and rare earth metal oxide,  $\text{CaAl}_2\text{O}_4$  (Lemonidou *et al.*, 1998) and  $\text{CeO}_2\text{-ZrO}_2$ . A promising catalyst system for the reforming reactions appeared to be a metal on  $\text{CeO}_2\text{-ZrO}_2$  support, where the metal can be Ni, Pt or Pd. Ni/ $\text{CeO}_2\text{-ZrO}_2$  has also been successfully applied to partial oxidation and autothermal reforming of methane.

It is well established that cerium oxide ( $\text{CeO}_2$ ) and ceria-zirconia ( $\text{CeO}_2\text{-ZrO}_2$ ) are useful in a wide variety of applications involving oxidation or partial oxidation of hydrocarbons (e.g. automotive catalysis) and as anodes for SOFC. This material has high oxygen storage capacity, which is beneficial in oxidation processes. The excellent resistance toward carbon formation from methane cracking reaction over  $\text{CeO}_2$  compared to commercial Ni/ $\text{Al}_2\text{O}_3$  was also reported recently (Laosiripojana, 2003). The addition of zirconium oxide ( $\text{ZrO}_2$ ) to cerium oxide ( $\text{CeO}_2$ ) has been found to improve the oxygen storage capacity, redox property, thermal stability, and catalytic activity (Ozawa *et al.*, 1993). However, some of the main limitations to apply  $\text{CeO}_2$  and  $\text{CeO}_2\text{-ZrO}_2$  in the high temperature steam reforming reaction are their low specific surface and their high surface area reduction percentage due to the high surface sintering (Laosiripojana, 2003). It was observed that the reduction for  $\text{CeO}_2$  and  $\text{CeO}_2\text{-ZrO}_2$  after exposure in methane steam reforming conditions at 900°C were 23% and 28%, respectively. The corresponding post-reaction specific surface areas were only 1.9 and 8.7  $\text{m}^2 \text{g}^{-1}$ , respectively (Laosiripojana, 2003).

The use of high surface area (HSA) ceria-based materials as the catalyst support would be a good alternative procedure to improve the methane steam reforming performance. Several methods have recently been described for the preparation of high surface area (HSA)  $\text{CeO}_2$  and  $\text{CeO}_2\text{-ZrO}_2$  solid solutions. Most interest is focused on the preparation of transition-metal oxides using templating pathways. Several meso-structured surfactant-oxide composites have been synthesized by this approach. However, only a few of these composites showed a regular pore structure after calcination. A surfactant-assisted approach was employed to prepare high surface area  $\text{CeO}_2$  and  $\text{CeO}_2\text{-ZrO}_2$  with improved textural, structural and chemical properties for environmental applications (Terribile *et al.*, 1998). They were prepared by react a cationic surfactant with a hydrous mixed oxide produced by co-precipitation under basic conditions. By this preparation procedure, the supports with good homogeneity and stability especially after thermal treatments were achieved.  $\text{CeO}_2\text{-ZrO}_2$  with the specific surface area higher than 230  $\text{m}^2 \text{g}^{-1}$  was obtained after calcination at 723 K. The value dropped to ca. 40  $\text{m}^2 \text{g}^{-1}$  after the following treatment at 1173 K.

In the present work, high surface area (HSA)  $\text{CeO}_2$  and  $\text{CeO}_2\text{-ZrO}_2$  were synthesized by the surfactant-assisted approach. Ni was selected as a metal catalyst and impregnated on these high surface area supports. For Ni/ $\text{CeO}_2\text{-ZrO}_2$ , different ratios of Ce/Zr were firstly investigated to determine a suitable catalyst composition. The stability and activity of Ni on high surface area  $\text{CeO}_2$  and  $\text{CeO}_2\text{-ZrO}_2$  were then studied and compared to Ni on low surface area  $\text{CeO}_2$  and  $\text{CeO}_2\text{-ZrO}_2$ , and also conventional Ni/ $\text{Al}_2\text{O}_3$ . The resistance toward carbon formation and the influences of possible inlet compositions of  $\text{CH}_4$ ,  $\text{H}_2$ ,  $\text{H}_2\text{O}$ , and  $\text{CO}_2$  on the methane steam reforming over these catalysts were also determined. In addition, the autothermal reforming, the combination between the steam reforming with the partial oxidation reaction in a single process, was investigated by adding oxygen the inlet feed.

## Experimental

### Material preparation and characterization

Low surface area (LSA)  $\text{CeO}_2\text{-ZrO}_2$  supports with different Ce/Zr molar ratios were prepared by co-precipitation of cerium chloride ( $\text{CeCl}_3 \cdot 7\text{H}_2\text{O}$ ), and zirconium oxychloride ( $\text{ZrOCl}_2 \cdot 8\text{H}_2\text{O}$ ) from Aldrich. The starting solution was prepared by mixing 0.1 M of metal salt solutions with 0.4 M of ammonia at a 2 to 1 volumetric ratio. This solution was stirred by magnetic stirring (100 rpm) for 3 h, then sealed and placed in a thermostatic bath maintained at  $90^\circ\text{C}$  for three days. The ratio between each metal salt was altered to achieve nominal Ce/Zr molar ratios of 1/3, 1/1 and 3/1. The precipitate was filtered and washed with deionised water and acetone to remove the free surfactant. It was dried overnight in an oven at  $110^\circ\text{C}$ , and then calcined in air at  $1000^\circ\text{C}$  for 6 h. Although, in these experiments, the sample abilities were tested at a temperature around  $900^\circ\text{C}$ , the calcination temperature actually comes from the real reforming temperature which can increase as high as  $1000^\circ\text{C}$ . So the surface area of the samples should also be estimate at  $1000^\circ\text{C}$ .

High surface area (HSA)  $\text{CeO}_2\text{-ZrO}_2$  supports were prepared by the surfactant-assisted method (Terribile *et al.*, 1998). An aqueous solution of an appropriate cationic surfactant and 0.1 M cetyltrimethylammonium bromide solution from Aldrich were added to an 0.1 M aqueous solution containing  $\text{CeCl}_3 \cdot 7\text{H}_2\text{O}$  and  $\text{ZrOCl}_2 \cdot 8\text{H}_2\text{O}$  in a desired molar ratio. The molar ratio of  $([\text{Ce}]+[\text{Zr}])/[\text{cetyltrimethylammonium bromide}]$  was kept constant at 0.8. The mixture was stirred and then aqueous ammonia was slowly added with vigorous stirring. The mixture was continually stirred for 3 h, then sealed and placed in the thermostatic bath maintained at  $90^\circ\text{C}$  for three days. After that, the mixture was cooled and the resulting precipitate was filtered and washed repeatedly with water and acetone. The filtered powder was dried in the oven at  $110^\circ\text{C}$  for one day and then calcined in air at  $1000^\circ\text{C}$  for 6 h.

Similarly,  $\text{CeO}_2$  (both high and low surface areas) were prepared using the same procedures

as  $\text{CeO}_2\text{-ZrO}_2$ , but without the addition of  $\text{ZrOCl}_2 \cdot 8\text{H}_2\text{O}$ .  $\text{Ni/CeO}_2\text{-ZrO}_2$ ,  $\text{Ni/CeO}_2$  and  $\text{Ni/Al}_2\text{O}_3$  with 5wt% Ni were prepared by impregnating the respective supports with  $\text{NiCl}_3$  solution at room temperature. These solutions were stirred by magnetic stirring (100 rpm) for 6 h. The solution was dried overnight in the oven at  $110^\circ\text{C}$ , and then calcined in air at  $1000^\circ\text{C}$  for 6 h. The catalysts were reduced with 10%  $\text{H}_2$  in Ar before use. The BET measurements of  $\text{CeO}_2$  and  $\text{CeO}_2\text{-ZrO}_2$  were carried out before and after the calcinations in order to determine the specific surface area.

In addition to the above characterizations, the redox properties of the catalysts were determined by the temperature programmed reduction (TPR) at high temperature. Regarding this experiment, 5%  $\text{H}_2/\text{Ar}$  was used, while the temperature of the system increased from room temperature to  $900^\circ\text{C}$ .

### Experimental set-up

Figure 1 shows the schematic diagram of the experimental reactor system. It consists of three main sections: feed, reaction, and analysis sections.

The main obligation of the feed section is to supply the components of interest such as  $\text{CH}_4$ ,  $\text{H}_2\text{O}$ ,  $\text{H}_2$ , or  $\text{O}_2$  to the reaction section, where an 8-mm internal diameter and 40-cm length quartz reactor was mounted vertically inside a furnace. The catalyst was loaded in the quartz reactor, which was already packed with a small amount of quartz wool to prevent the catalyst from moving. The residence time was kept constant at  $5 \times 10^{-4}$  g min  $\text{cm}^{-3}$ . The weight of catalyst loading was 10-100 mg, while a typical range of total gas flow was 20-200 ml/min depending on the desired gas velocity. The gas mixture flowed through the catalyst bed in the quartz reactor. A type-K thermocouple was inserted into the annular space between the reactor and the furnace. The thermocouple was mounted on the reactor in close contact with the catalyst bed to minimize the temperature difference between the catalyst bed and the thermocouple. After the reactions, the exit gas was transferred via trace-heated lines to the analysis section, which consists of a Porapak Q column Shimadzu 14B gas chro-

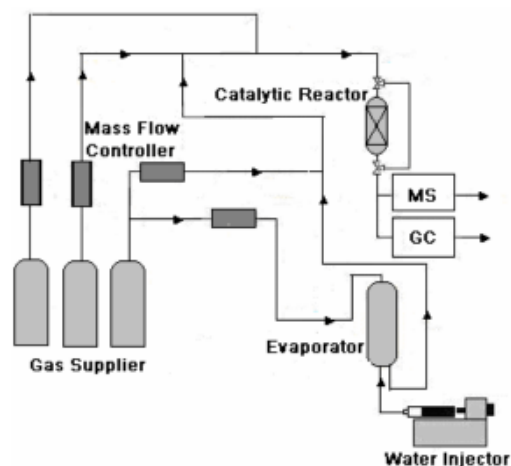


Figure 1. Schematic diagram of the experimental set-up.

matography (GC) and a mass spectrometer (MS). The gas chromatography was applied in order to investigate the steady state condition experiments, whereas the mass spectrometer was used for the transient and carbon formation experiments. In addition, the mass spectrometer was also applied together with the gas chromatography in order to investigate the effect of  $O_2$  partial pressure on the steam reforming rate, as an  $O_2$  peak in the chromatogram (TCD detector) occurred at the same retention time as a CO peak.

In the present work, the outlet of the GC column was directly connected to a thermal conductivity detector (TCD). In order to satisfactorily separate  $CH_4$ , CO,  $CO_2$ , and  $H_2O$ , the temperature setting inside the GC column was programmed varying with time. In the first 3 min, the column temperature was constant at  $60^\circ C$ . Then, it was

increased steadily by the rate of  $15^\circ C$  per min until  $120^\circ C$ . Finally, the temperature was decreased to  $60^\circ C$ . The analytical method applied is an internal standardization. The peak area is related to the molar concentration through the response factor (RF).

$$RF = \frac{\text{concentration (ppm)}}{\text{peak area}}$$

Table 1 presents the absolute response factor (RF) for all components concerned in this research. In order to study the formation of carbon species on catalyst surface, the transient exit gas from the catalytic reactor was analyzed using the mass spectrometer. Sampling of the exit gas was done by a quartz capillary and differential pumping. The calibrations of CO and  $CO_2$  were performed by injecting a known amount of these

Table 1. Absolute response factors and retention time of each component

Gas	RF	Retention time
$H_2$	0.35	0.7
$O_2$	0.28	1.11
CO	0.19	1.15
$CH_4$	0.09	1.59
$CO_2$	0.21	2.65
$H_2O$	0.17	5.5

calibration gases from a loop in an injection valve in the bypass line. The response factors were obtained by dividing the number of moles for each component over the respective areas under peaks. This process was performed before each experiment to achieve maximum accuracy in the quantitative carbon analysis.

### Temperature programmed techniques (TP)

In the present work, temperature programmed technique (TP) was applied for studying carbon formation and water gas shift reaction experiments. Temperature Programmed Methane Adsorption (TPMA) was done in order to investigate the reaction of methane with the surface of catalyst. 5% Methane in helium with the total flow rate of 100 ml min<sup>-1</sup> was introduced into the system, while the operating temperature increased from room temperature to 900°C by the rate of 10°C/min. Then, the system was cooled down to the room temperature under helium flow. After the TPMA experiment, the carbon deposited on the catalyst was investigated by the temperature programmed oxidation (TPO). 10% Oxygen in helium with the total flow rate of 100 ml min<sup>-1</sup> was introduced into the system, after a He purge. Similar to TPMA, the temperature was increased from room temperature to 900°C at the rate of 10°C/min.

In addition, the temperature programmed reaction (TPRx) of CO/H<sub>2</sub>O/He gas mixture was also carried out in order to investigate the water

gas shift reaction. The mixture of 5%CO and 10% H<sub>2</sub>O in helium was introduced into the system during heating up period by the rate of 10°C/min before reaching the isothermal condition at 900°C.

## Results

### 1. Investigate surface area by BET (Brunauer-Emmett-Teller)

The BET measurements of CeO<sub>2</sub> and CeO<sub>2</sub>-ZrO<sub>2</sub> were carried out before and after the calcinations in order to determine the specific surface area. The values are presented in Table 2. After drying in oven, surface areas of 105 and 115-135 m<sup>2</sup> g<sup>-1</sup> were observed for high surface area CeO<sub>2</sub> and CeO<sub>2</sub>-ZrO<sub>2</sub> (with different Ce/Zr ratio), respectively and, as expected, the surface area dramatically decreased at high calcination temperatures. However, the values are still appreciable after calcination at 1000°C. By using the surfactant-assisted method, CeO<sub>2</sub> and CeO<sub>2</sub>-ZrO<sub>2</sub> with high surface area of 29 and 40-42 m<sup>2</sup> g<sup>-1</sup>, respectively, after calcination at 1000°C were obtained. They are 2-3 times higher than those of low surface area supports. It should be noted that the introduction of ZrO<sub>2</sub> can stabilize the surface area of ceria, which is in good agreement with the results obtained on catalysts prepared by conventional routes (Lao-siripojana, 2003). This is probably due to the inhibition of the sintering process induced by the dopant ion (Terribile *et al.*, 1998).

**Table 2. Surface area of the support before and after calcination at 1000°C**

Catalysts	Surface area before calcination(m <sup>2</sup> g <sup>-1</sup> )	Surface area after calcination at 1000°C(m <sup>2</sup> m <sup>2</sup> g <sup>-1</sup> )
ZrO <sub>2</sub> (HSA)	147	47
CeO <sub>2</sub> -ZrO <sub>2</sub> (HSA)(Ce/Zr = 1/3)	135	42
CeO <sub>2</sub> -ZrO <sub>2</sub> (HSA)(Ce/Zr = 1/1)	120	41
CeO <sub>2</sub> -ZrO <sub>2</sub> (HSA)(Ce/Zr = 3/1)	115	40
CeO <sub>2</sub> (HSA)	105	24
ZrO <sub>2</sub> (LSA)	94	31
CeO <sub>2</sub> -ZrO <sub>2</sub> (LSA)(Ce/Zr = 1/3)	82	20
CeO <sub>2</sub> -ZrO <sub>2</sub> (LSA)(Ce/Zr = 1/1)	74	18
CeO <sub>2</sub> -ZrO <sub>2</sub> (LSA)(Ce/Zr = 3/1)	70	19
ZrO <sub>2</sub> (LSA)	55	8.5

## 2. Investigation of the redox properties and redox reversibility of the catalysts

As described earlier, the oxygen storage capacities and the degree of redox properties for catalysts were investigated by using temperature programmed reduction (TPR) due to the amount of hydrogen uptake relates to the amount of free oxygen on the surface of the particles. TPR was done by introducing 5%  $H_2$  in argon while heating the system up to 900°C and the results of hydrogen uptakes from the mass spectrometer signal (a.u.) were detected from varieties ratio of Ce/Zr including pure  $ZrO_2$ , Ce/Zr = 1/1, 1/3 and 3/1 as shown in Figure 2. From this experiment, the amount of hydrogen uptake significantly decreased for samples which included more Ce, whereas no hydrogen uptakes were observed from pure  $ZrO_2$ .

The results indicated that, according to these experimental conditions, the occurrence of redox properties for samples which have the combination with the Ce/Zr have much more activity than the pure ceria and these properties were decreased when Ce content increased. For comparison, the redox properties of samples when prepared by different methods, the amount of hydrogen uptakes of  $CeO_2$  and  $CeO_2-ZrO_2$  (1/3 ratios of Ce/Zr) samples were studied.

As presented in Figure 3, the amount of hydrogen uptakes of 1/3 ratio of Ce/Zr sample prepared by surfactant assisted method was significant higher than the other samples while pure ceria prepared by precipitation method had the lowest amount of hydrogen consumption.

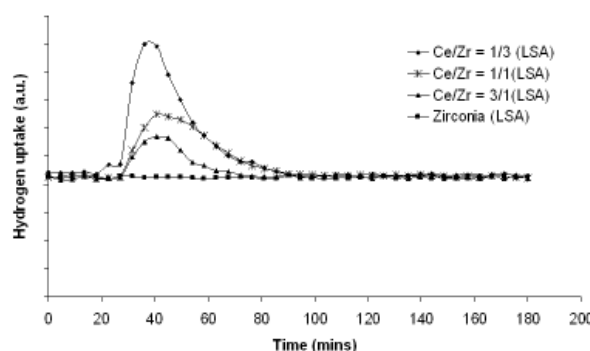


Figure 2. Temperature Programmed Reduction (TPR) of  $CeO_2-ZrO_2$  prepared by precipitation method in the different ratio of Ce/Zr

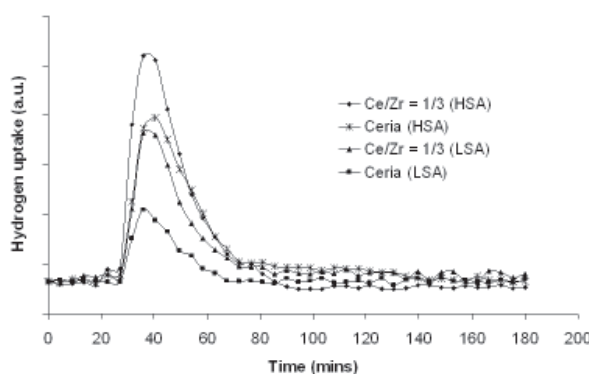


Figure 3. Temperature Programmed Reduction (TPR) of  $CeO_2$  and 1/3 ratio of Ce/Zr sample prepared by precipitation method (LSA) and surfactant assisted method (HSA)

### 3. Methane steam reforming reactivity for Ni/CeO<sub>2</sub>-ZrO<sub>2</sub> with different Ce/Zr

Ni/CeO<sub>2</sub>-ZrO<sub>2</sub> catalysts with different Ce/Zr ratios (1/3, 1/1, and 3/1) were firstly tested in methane steam reforming conditions at 900°C for both high (HSA) and low (LSA) surface areas in order to select the most suitable ratio of Ce/Zr for the main studies. The results shown in Figure 4 revealed that at steady state, Ni/CeO<sub>2</sub>-ZrO<sub>2</sub> with Ce/Zr ratio of 3/1 shows the best performance in terms of stability and activity for both high and low surface areas. It should be noted that the reforming activities in that figure are presented as the relative reforming activity, which is calculated from comparing the amount of the methane conversion at that point with the greatest value in the experiment. According to these experimental results, Ni/CeO<sub>2</sub>-ZrO<sub>2</sub> with Ce/Zr ratio of 3/1 was selected for further investigations.

### 4. Stability and activity of several catalysts toward methane steam reforming

In order to study the influence of high surface area (HSA) ceria-based supports, Ni/CeO<sub>2</sub> (HSA) and Ni/CeO<sub>2</sub>-ZrO<sub>2</sub> (HSA) were tested and the performances were compared with general metal-support catalysts including Ni/Al<sub>2</sub>O<sub>3</sub>, Ni/CeO<sub>2</sub>-ZrO<sub>2</sub> (LSA) and Ni/CeO<sub>2</sub> (LSA) (low specific surface area CeO<sub>2</sub> and CeO<sub>2</sub>-ZrO<sub>2</sub>). The inlet components were CH<sub>4</sub>/H<sub>2</sub>O/H<sub>2</sub> in helium with the inlet

ratio of 1.0/3.0/0.2. The main products from the reactions over these catalysts were H<sub>2</sub> and CO with some CO<sub>2</sub>, indicating a contribution from the water-gas shift, and the reverse methanation at this high temperature. The steam reforming rate was measured as a function of time in order to indicate the stability and the deactivation rate. The variations in relative reforming activity with time for different catalysts are shown in Figure 5. At steady state, Ni/CeO<sub>2</sub> (HSA) and Ni/CeO<sub>2</sub>-ZrO<sub>2</sub> (HSA) presented much higher reactivity toward the methane steam reforming than Ni/Al<sub>2</sub>O<sub>3</sub>, Ni/CeO<sub>2</sub>-ZrO<sub>2</sub> (LSA), and Ni/CeO<sub>2</sub> (LSA).

The steam reforming activities of Ni/CeO<sub>2</sub> (LSA) and Ni/Al<sub>2</sub>O<sub>3</sub> significantly declined with time before reaching a new steady-state rate at a much lower value, while the activity of Ni/CeO<sub>2</sub> (HSA), Ni/CeO<sub>2</sub>-ZrO<sub>2</sub> (HSA), and Ni/CeO<sub>2</sub>-ZrO<sub>2</sub> (LSA) declined slightly. Catalyst stabilities expressed as a deactivation percentage are given in Table 3 where the deactivation percentages are the percentage of the methane conversion decreasing at the reaction time. In order to investigate the reason of the catalyst deactivation, the post-reaction temperature-programmed oxidation (TPO) experiments were then carried out. TPO experiments detected no carbon formation on the surface of Ni on ceria-based supports. In contrast, the quantities of carbon deposited on the surface of Ni/Al<sub>2</sub>O<sub>3</sub> were 1.35 monolayers.

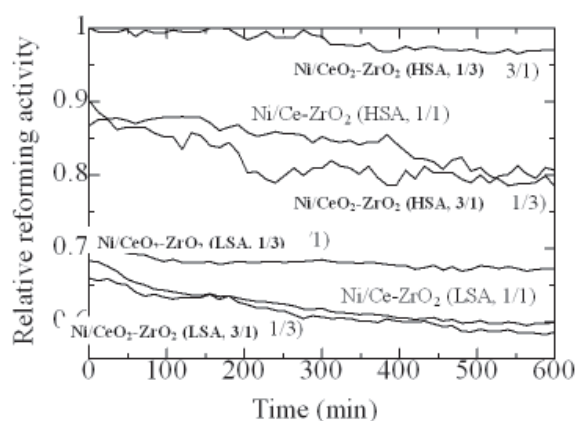


Figure 4. Methane steam reforming of the different ratio of Ce/Zr and different preparation method at operation temperature 900°C



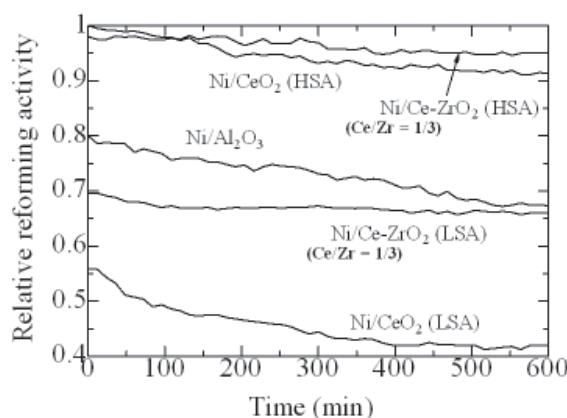


Figure 5. Methane steam reforming activity of different kinds of catalyst at 900°C

Table 3. Specific surface area of the catalysts before and after reaction.

Catalysts	Deactivation (%)	Specific surface area before and after reaction ( $\text{m}^2 \text{g}^{-1}$ )	Surface area reduced (%)
Ni/CeO <sub>2</sub> (HSA)	8.7	24 and 22	8.3
Ni/CeO <sub>2</sub> -ZrO <sub>2</sub> (HSA) (Ce/Zr = 1/3)	7	42 and 39	7.1
Ni/CeO <sub>2</sub> -ZrO <sub>2</sub> (HSA) (Ce/Zr = 1/1)	12	41 and 36	12
Ni/CeO <sub>2</sub> -ZrO <sub>2</sub> (HSA) (Ce/Zr = 3/1)	3	40 and 39	2.5
Ni/CeO <sub>2</sub> (LSA)	24	8.5 and 6.2	27
Ni/CeO <sub>2</sub> -ZrO <sub>2</sub> (LSA) (Ce/Zr = 1/3)	11	20 and 18	10
Ni/CeO <sub>2</sub> -ZrO <sub>2</sub> (LSA) (Ce/Zr = 1/1)	12	18 and 15	13
Ni/CeO <sub>2</sub> -ZrO <sub>2</sub> (LSA) (Ce/Zr = 3/1)	5.1	19 and 18	4.5
Ni/Al <sub>2</sub> O <sub>3</sub>	16	40 and 40	~0

The BET measurement, as presented in Table 3, suggested that the deactivations of Ni/CeO<sub>2</sub> and Ni/CeO<sub>2</sub>-ZrO<sub>2</sub> were mainly due to the reduction of surface area. However, the reduction percentages of Ni/CeO<sub>2</sub> (HSA) and Ni/CeO<sub>2</sub>-ZrO<sub>2</sub> (HSA) are lower than those with low surface area, indicating the high stability of CeO<sub>2</sub> (HSA) and CeO<sub>2</sub>-ZrO<sub>2</sub> (HSA) toward the thermal sintering. It should be noted that although Ni/Al<sub>2</sub>O<sub>3</sub> was thermally stable at high operating temperature, it was more susceptible to carbon formation which led to the catalyst deactivation.

### 5. Resistance toward carbon formation

The resistances of Ni/CeO<sub>2</sub> (HSA) and Ni/CeO<sub>2</sub>-ZrO<sub>2</sub> (HSA) toward the formation of carbon

species were investigated and compared to other Ni catalysts on low surface area (LSA) ceria-based supports, and also Ni/Al<sub>2</sub>O<sub>3</sub>. The temperature programmed techniques; i.e., TPMA and TPO, were carried out. The former is for determining the reaction between methane and the catalyst surface while the latter is for determining the amount of carbon deposited on the catalyst. Figure 6 presents the TPMA results for Ni/CeO<sub>2</sub>-ZrO<sub>2</sub> (LSA), Ni/CeO<sub>2</sub> (HSA) and Ni/CeO<sub>2</sub>-ZrO<sub>2</sub> (HSA), while Figure 7 presents the TPO results for those catalysts and Ni/Al<sub>2</sub>O<sub>3</sub>.

As seen in Figure 6, carbon monoxide and carbon dioxide were also produced together with hydrogen for Ni catalysts on ceria-based supports due to the gas-solid reaction of CH<sub>4</sub> on Ce<sup>4+</sup>,

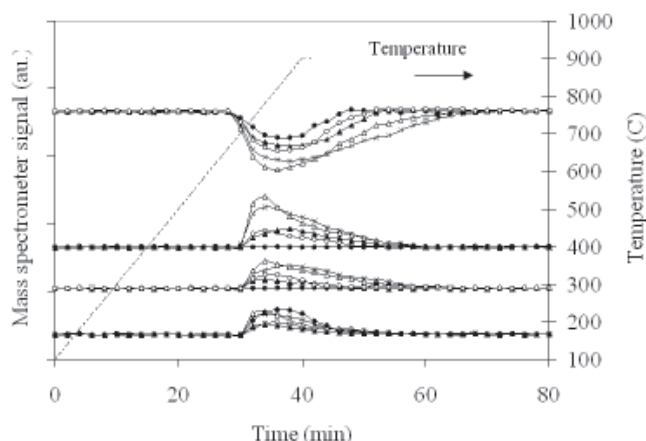


**Figure 6. Temperature Programmed Methane Adsorption (TPMA) over  $\Delta$  Ni/CeO<sub>2</sub>-ZrO<sub>2</sub> (HSA),  $\times$  Ni/CeO<sub>2</sub> (HSA),  $\circ$  Ni/CeO<sub>2</sub>-ZrO<sub>2</sub> (LSA),  $\blacktriangle$  Ni/CeO<sub>2</sub> (LSA), and  $\bullet$  Ni/Al<sub>2</sub>O<sub>3</sub>**

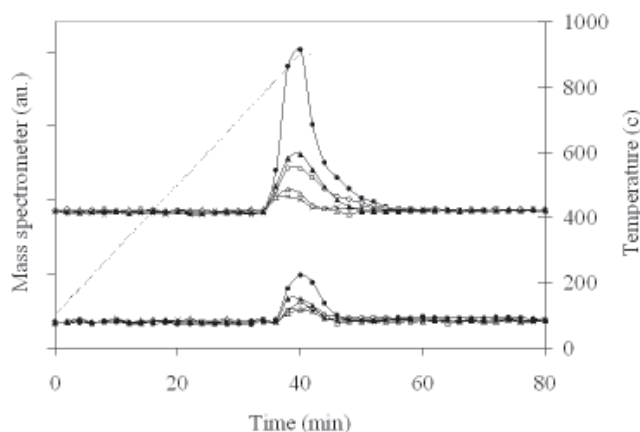


**Figure 7. Temperature Programmed Oxidation over  $\Delta$  Ni/CeO<sub>2</sub>-ZrO<sub>2</sub> (HSA),  $\times$  Ni/CeO<sub>2</sub> (HSA),  $\circ$  Ni/CeO<sub>2</sub>-ZrO<sub>2</sub> (LSA),  $\blacktriangle$  Ni/CeO<sub>2</sub> (LSA), and  $\bullet$  Ni/Al<sub>2</sub>O<sub>3</sub> at 900°C**

whereas only hydrogen peak was detected for TPMA over Ni/Al<sub>2</sub>O<sub>3</sub>. According to Figure 7, the gas-solid reactions of methane on Ni/CeO<sub>2</sub> (HSA) and Ni/CeO<sub>2</sub>-ZrO<sub>2</sub> (HSA) were significantly higher than that on Ni/CeO<sub>2</sub>-ZrO<sub>2</sub> (LSA). The amount of carbon formation on the surface of each catalyst was then determined by measuring the CO and CO<sub>2</sub> yield obtained from the TPO results. Using a value of 0.026 nm<sup>2</sup> for the area occupied by a carbon atom in a surface monolayer of the basal plane in graphite (Otsuka *et al.*, 1985), the quantities of carbon deposited on the surface of each catalyst at different temperatures were determined

(Table 4). Clearly, Ni/CeO<sub>2</sub> (HSA) and Ni/CeO<sub>2</sub>-ZrO<sub>2</sub> (HSA) provided higher resistance toward carbon formation than Ni/Al<sub>2</sub>O<sub>3</sub>, Ni/CeO<sub>2</sub>-ZrO<sub>2</sub> (LSA), and Ni/CeO<sub>2</sub> (LSA).

### Discussion

According to the redox testing, CeO<sub>2</sub>-ZrO<sub>2</sub> prepared by surfactant assisted method with the ratio of Ce/Zr 1/3 provided the greatest ability of redox properties compared to those from other experimental candidates. This is mainly due to the relation between the specific surface area of

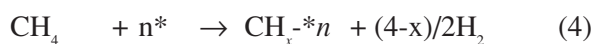
**Table 4.** Amount of carbon remaining on catalyst surface after dry reforming of methane (0.05 atm CH<sub>4</sub>, and without H<sub>2</sub>O)

Catalysts	Amount of carbon deposition (monolayers)				
	900°C	925°C	950°C	975°C	1000°C
Ni/CeO <sub>2</sub> (HSA)	0.9	1.35	1.77	2.09	2.44
Ni/CeO <sub>2</sub> -ZrO <sub>2</sub> (HSA)	1.04	1.42	1.84	2.16	2.53
Ni/CeO <sub>2</sub> (LSA)	1.25	1.78	2.27	2.89	3.42
Ni/CeO <sub>2</sub> -ZrO <sub>2</sub> (LSA)	1.29	1.8	2.33	2.94	3.47
Ni/Al <sub>2</sub> O <sub>3</sub>	2.35	3.47	4.64	5.83	6.98

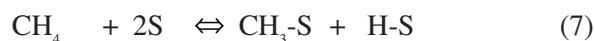
material and the redox properties. According to the experiment, adding ZrO<sub>2</sub> provided higher surface area than those from pure CeO<sub>2</sub> and led to the high hydrogen uptake during the TPR testing, which means the increasing of oxygen storage capacity. It should be noted that although pure ZrO<sub>2</sub> has the highest specific surface area, the hydrogen uptake during the TPR is 0, which is due to the zero oxygen storage capacity of ZrO<sub>2</sub>.

Improvements of stability and activity toward methane steam reforming were achieved for Ni on high surface area (HSA) ceria-based supports. The higher stabilities are due to the lower surface area reduction percentage compared to Ni on low surface area (LSA) ceria-based supports, while the higher reforming activities of Ni/CeO<sub>2</sub> (HSA) and Ni/CeO<sub>2</sub>-ZrO<sub>2</sub> (HSA) is possibly due to the improvement of Ni dispersion on the high surface area support, and also the increasing in solid-gas reaction between the high surface area (HSA) ceria-based supports and CH<sub>4</sub>.

Regarding the well known methane steam reforming mechanism over conventional Ni catalyst proposed by (Dicks *et al.*, 2000), methane will only adsorb on the active surface site of Ni (\*) and forms CH<sub>x</sub>-\*n. Simultaneously, the adsorption of inlet steam also takes place on the surface site of Ni catalyst forming O-\*. These elements, O-\* and CH<sub>x</sub>-\*n, eventually reacts each other producing CO and H<sub>2</sub>, and also recovers the active surface site of Ni (\*) as illustrated below.



For the steam reforming of methane over Ni/CeO<sub>2</sub>-ZrO<sub>2</sub>, in addition to the reactions on Ni surface, the redox reaction between inlet CH<sub>4</sub> and the lattice oxygen (O<sub>x</sub>) on CeO<sub>2</sub>-ZrO<sub>2</sub> surface will also take place producing H<sub>2</sub> and CO. Moreover, the reduced CeO<sub>2</sub>-ZrO<sub>2</sub> can react with inlet H<sub>2</sub>O to produce more H<sub>2</sub> and recover O<sub>x</sub> (Laosiripojana *et al.*, 2005). The proposed mechanism for these redox reactions, involving the reactions between methane and/or an intermediate surface hydrocarbon species with the lattice oxygen (O<sub>x</sub>) on CeO<sub>2</sub>-ZrO<sub>2</sub> surface and the recovery of O<sub>x</sub> by steam, is presented schematically below.



The surface site (S) can be either a unique site, or can also be considered to be the same site as the catalyst oxidized site ( $O_x$ ) (Laosiripojana *et al.*, 2005). It has been reported that the controlling step of these redox reactions is the reaction of methane on  $CeO_2$ - $ZrO_2$  surface; in addition, the lattice oxygen is replenished by a significant rapid surface reaction of the reduced state  $CeO_2$ - $ZrO_2$  with  $H_2O$ .

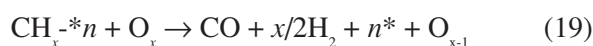
According to the possible formation of carbon species on the surface of catalyst during the steam reforming process, the following reactions are theoretically the most probable reactions that could lead to carbon formation:



C is the carbonaceous deposits. Reactions (16-17) are favorable at low temperature, while reaction (14-15) is thermodynamically unflavored (Dicks *et al.*, 2000). At such a high temperature, the Boudard reaction (Eq. 14) and the decomposition of methane (Eq. 15) are the major pathways for carbon formation as they show the largest change in Gibbs energy (Aguiar *et al.*, 2004).

In the present work, we also observed high amount of carbon formation on the surface of Ni/ $Al_2O_3$  after exposure in methane steam reforming condition. By applying  $CeO_2$ - $ZrO_2$  as support, the formation of carbon species could be inhibited by the redox reactions of methane and carbon monoxide (produced during the steam reforming process) with the lattice oxygen ( $O_x$ ) at  $CeO_2$ - $ZrO_2$  surface forming hydrogen and carbon dioxide, which is thermodynamically unflavored to form carbon species in this range of conditions. Therefore, significantly lower amounts of carbon deposition were consequently observed for Ni/ $CeO_2$ - $ZrO_2$ . In addition, the reaction between the lattice oxygen ( $O_x$ ) at  $CeO_2$ - $ZrO_2$  surface with the

adsorbed methane on Ni surface ( $CH_x^{*n}$ ) and the rapid recovery of the lattice oxygen by the simultaneous supply of oxygen from  $H_2O$  also result in the higher resistance toward carbon formation and less inlet  $H_2O/CH_4$  requirement for Ni/ $CeO_2$ - $ZrO_2$ .



## Conclusion

High surface area  $CeO_2$  and  $CeO_2$ - $ZrO_2$  with Ce/Zr ratio of 3/1 are the good candidates to be used as the support for Ni catalysts for reforming methane and producing hydrogen for later utilization in SOFC. The great advantages of using Ni on high surface area (HSA) ceria-based supports are the high reforming reactivity, and also the high stability due to their excellent resistance toward carbon formation even at such a high temperature (900°C). Ni/ $CeO_2$  (HSA) and Ni/ $CeO_2$ - $ZrO_2$  (HSA) with Ce/Zr = 3/1 provided the same range of stability and activity toward the methane steam reforming.

## Acknowledgement

The financial support from The Joint Graduate School of Energy and Environment (JGSEE), The Thailand Research Fund (TRF), and MTEC throughout this project is gratefully acknowledged.

## References

- Aguiar, P., Chadwick, D. and Kershenbaum, L. 2004. Effect of methane slippage on an indirect internal reforming solid oxide fuel cell, *Chem. Eng. Sci.*, 59: 87-97.
- Dicks, A.L., Pointon, K.D. and Siddle, A.J. 2000. Intrinsic reaction kinetics of methane steam reforming on a nickel/zirconia anode, *Power Sources*, 86: 523-530.
- Laosiripojana, N. 2003. Reaction engineering of indirect internal steam reforming of methane for application in solid oxide fuel cells, Ph.D. Thesis, University of London, England.

- Laosiripojana, N. and Assabumrungrat, S. 2005. Methane steam reforming over Ni/Ce-ZrO<sub>2</sub> catalyst: Influences of Ce-ZrO<sub>2</sub> support on reactivity, resistance toward carbon formation, and intrinsic reaction kinetics, *Applied Catalysis A: General*, 290: 200-211.
- Lemonidou, A.A., Goula, M.A. and Vasalos, I.A. 1998. Carbon dioxide reforming of methane over 5 wt.% nickel calcium aluminate catalysts - effect of preparation method, *Catal. Today*, 46: 175-183.
- Otsuka, K., Hatano, M. and Morikawa, A. 1985. Decomposition of water by cerium oxide of  $\delta$ -phase, *Inorganica Chimica Acta.*, 109: 193.
- Ozawa, M., Kimura, M. and Isogai, A. 1993. The application of Ce--Zr oxide solid solution to oxygen storage promoters in automotive catalysts, *J. Alloys Comp.*, 193: 73.
- Terribile, D., Trovarelli, A., Llorca, J., Leitenburg, C. de and Dolcetti, G. 1998. The preparation of high surface area CeO<sub>2</sub>-ZrO<sub>2</sub> mixed oxides by a surfactant-assisted approach, *Catal. Today*, 43: 79-88.
- Wang, X. and Gorte, R.J. 2002. A study of steam reforming of hydrocarbon fuels on Pd/ceria, *Appl. Catal. A*, 224: 209-218.